Transit-Time Effects in the Noise of Schottky-Barrier Diodes

MICHAEL TRIPPE, MEMBER, IEEE, GIJS BOSMAN, MEMBER, IEEE, AND ALDERT VAN DER ZIEL, LIFE FELLOW, IEEE

Abstract —**Room-temperature noise measurements at 2.2, 12, and 97.5 GHz were performed on commercial silicon Schottky-barrier diodes and are shown to agree with the model presented in this work. This model is an extension of earlier work by van der Ziel on infrared detection in Schottky-barrier diodes. In the theoretical analysis, the electrons participating in the charge-transport process across the barrier are subdivided into four groups based on their initial velocity. The contribution of each group to the device conductance, susceptance, and current spectral intensity was incorporated, including the effects of the transit time. By taking each of these effects into account, an accurate model which applies over a wide range of bias and frequency has been developed. Although the emphasis of this model has been on the high-frequency performance, the model also gives the correct results in the low-frequency limit.**

I. Introduction

SCHOTTKY-BARRIER DIODES have become increasingly important due to their excellent high-frequency properties. They are in widespread use in the mixing and direct detection of signals at frequencies up to several hundred gigahertz [1]. Since these devices are being operated at such high frequencies, it is necessary to have a model which is capable of describing the device behavior on time scales on the order of the transit time of electrons across the junction. This paper presents such a model for silicon Schottky-barrier diodes and compares the theory with experimental results for commonly used commercial silicon devices. The theory is also applicable to GaAs devices, although in that case the effects will be less pronounced in the frequency range we consider in this paper due to the smaller effective mass of electrons in GaAs.

The noise characteristics indicate that three frequency regimes must be considered. At low frequencies, excess noise is dominant, which has a $1/f$ spectral dependence. In the intermediate-frequency range, the noise is white and is adequately explained by the well-known shot noise theory. At high frequencies, transit-time effects cause the noise to be a function of frequency.

Manuscript received December 18, 1985; revised June 9, 1986. This work was supported in part by the National Science Foundation under Grant No. ECS-8007623.

M. Trippe was with the Department of Electrical Engineering, University of Florida, Gainesville. He is now with Martin Marietta Research Laboratory, 1450 South Rolling Rd., Baltimore, MD 21227.

G. Bosman and A. van der Ziel are with the Department of Electrical Engineering, University of Florida, Gainesville, FL 32611.

IEEE Log Number 8610508.

II. Physical Model

In their basic form, Schottky-barrier diodes have a very simple configuration. This is depicted in Fig. 1. A small metal anode contact (e.g., gold) is deposited on top of a semiconducting wafer (e.g., Si or GaAs). A large-area ohmic back contact is used in order to lower the series resistance of the bulk semiconductor.

In spite of the simple configuration of Schottky-barrier diodes, the physical mechanisms which govern their operation are complex. The importance of each mechanism may also vary with frequency and bias.

The device description starts with a consideration of the band diagram (Fig. 2). The metal on the n-semiconductor gives an energy barrier of $q\Phi_{ms}$. The value of $q\Phi_{ms}$ is often calculated for metal–semiconductor systems by considering the work functions, electron affinities, and doping densities of the materials. This calculated value may be of little use as the actual barrier height also depends on the number of interface states, and this number may not be well controlled. In practice, the actual barrier height is determined from $I-V$ measurements once the reverse saturation current is known. This eliminates the need for assumptions concerning the metal–semiconductor barrier height. It will be assumed that the Schottky-barrier height remains constant with bias.

The difference in energy between the conduction band and Fermi level (far from the junction region) is qV_n. This is governed by the doping density in the semiconductor material and may be found from [2]

$$V_n = V_T \ln\left(\frac{N_C}{N_D}\right) \tag{1}$$

where V_T is the thermal voltage ($=kT/q$), which is equal to 25.8 mV at room temperature, N_C is the effective density of states of the conduction band, and N_D is the doping density.

Once $q\Phi_{ms}$ and qV_n have been determined, the diffusion potential V_{dif} may easily be found

$$V_{\text{dif}} = \Phi_{ms} - V_n. \tag{2}$$

This will be a convenient quantity for many calculations.

The charge-transport mechanism which governs the operation of the high-frequency Schottky-barrier diodes which we have studied is thermionic emission. In order for thermionic emission to dominate the dc current, the depletion

0018-9480/86/1100-1183$01.00 ©1986 IEEE

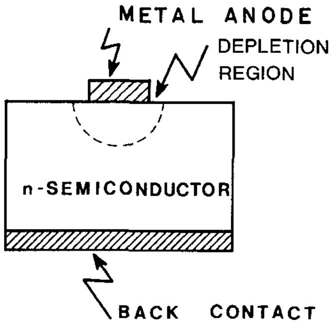

Fig. 1. Configuration of a simple Schottky-barrier diode.

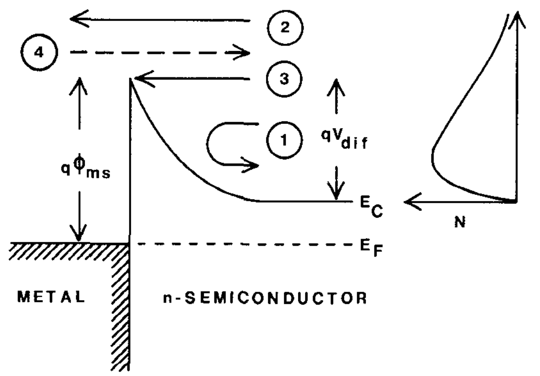

Fig. 2. Band diagram of the metal–semiconductor contact. Electrons of group 1 have KE $< qV_{dif}$ and return to the neutral semiconductor. Electrons of group 3 have KE $\simeq qV_{dif}$. Electrons of group 2 have KE $> qV_{dif}$ and always reach the metal contact. Electrons of group 4 make up the reverse saturation current.

region width must lie within a range of values; that is, the doping density should not be so low that significant scattering could occur in the space-charge region. In this work, it will be assumed that electrons can cross the space-charge region without suffering any scatterings. Conversely, the doping should not be high enough to allow the tunneling of electrons across the resultant narrow space-charge region.

According to Sze [2], the dc current flow will be due to thermionic emission if the electric field is between 10^4 V/cm and 10^5 V/cm in silicon diodes. This is the case for the assumed doping density of $10^{17}\,\text{cm}^{-3}$ of our diodes.

The process of thermionic emission is the thermal excitation of charge carriers to a sufficient kinetic energy such that they may cross the energy barrier of the junction. Since the bottom of the conduction band represents zero kinetic energy, electrons in the semiconductor must have at least an energy of qV_{dif} in the negative x direction in order to reach the metal contact and be collected.

The electrons of the semiconductor participating in the charge transport can be subdivided into four groups. (See Fig. 2.)

Electrons of group 1 have insufficient kinetic energy in the negative x direction (KE $< qV_{dif}$). These electrons always return to the neutral semiconductor and give no contribution to the dc current. These electrons have the same characteristic time of flight regardless of their initial velocity. At low frequencies, these electrons give no contribution to the device conductance. As the operating frequency increases, the small-signal conductance and noise due to these electrons rises as ω^2 and dominates the device conductance. It will be shown that this group of electrons controls the high-frequency behavior of the device at low biases. The conductance and noise of this group of electrons does not change significantly with bias. Most electrons of the semiconductor occupy states near the bottom of the conduction band; consequently, a change in the barrier height due to an applied voltage will not cause any appreciable change in the number of electrons in this group.

The electrons of group 3 have sufficient kinetic energy to just reach the metal contact (KE $\simeq qV_{dif}$). If no signal were applied, then these electrons would always be collected at the metal contact. With an applied small-signal voltage, some electrons of this group will be collected while others will return to the neutral semiconductor. For this group of electrons, dI/dV is large. At intermediate frequencies, this group of electrons dominates the small-signal device conductance, even though only a fraction of the dc current is carried by them. The conductance due to this group of electrons is constant up to frequencies on the order of the reciprocal transit time and decreases rapidly at higher-frequencies. The intermediate-frequency conductance of this group of electrons is given by the slope of the $I-V$ characteristic.

The electrons of the semiconductor which have sufficient velocity (kinetic energy) to always pass the energy barrier are designated as belonging to group 2, as shown in Fig. 2. Since the electrons of this group are always collected, they give rise to the dc current. With an applied signal, the velocity of the electrons during the transit time is slightly modulated. This is a small effect and the quantity dI/dV is approximately zero for this group. The contribution to the conductance from this group of electrons may be neglected for all frequencies of interest.

Group 3 is a special case of group 2 under ac short-circuited conditions. The same description will hold for both in calculating the spectral intensity of the noise. These electrons carry the dc current and, since the electrons are emitted at random times, give an intermediate-frequency spectral intensity equal to the shot noise of the dc current. The spectral intensity is white up to frequencies on the order of the reciprocal transit time and drops steeply at higher frequencies. This noise component varies linearly with the device current (exponentially with voltage). At high bias, the passing electrons will dominate.

The fourth group of electrons to be included consists of electrons making up the reverse saturation current. The reverse saturation current consists of electrons in the metal which have sufficient kinetic energy in the positive x direction to cross the energy barrier of $q\Phi_{ms}$. Once the electrons have crossed the energy barrier, they are swept by the electric field to the neutral semiconductor. Since the electric field causes the electrons to be accelerated to a very high velocity, their transit time is extremely short. For this reason, the spectral intensity due to these electrons is considered white and equal to full-shot noise. The energy barrier $q\Phi_{ms}$ is not a function of bias in this model. This allows the magnitude of the reverse saturation current to be considered constant.

III. $I-V$ Characteristics of Schottky-Barrier Diodes

The current-transport mechanism which will be considered is the thermionic emission of electrons. The results of this model have been known for many years [3]. Some background information will be presented in order to show the assumptions invoked, but the reader is referred to the references for complete details.

The calculation of the $I-V$ characteristic is simplified by the fact that only electrons of groups 2 and 3 contribute to the dc current. Thus, it is only necessary to find the number of electrons traveling from the semiconductor to the metal per unit time. This current is a function of the applied bias voltage.

The current which is flowing may be expressed as an integral over the x-directed velocity. This may be shown to equal

$$I = \text{Area}\frac{4\pi q m^{*2} k}{h^3} T \int_{v_{00}}^{\infty} v_x \exp\left(\frac{-\frac{1}{2}m^* v_x^2}{kT}\right) dv_x \quad (3)$$

where v_{00} is the electron escape velocity. The integration over the v_y and v_z components has already been performed in (3). The integration variable may be changed by realizing that the condition for thermionic emission is

$$q(V_{\text{dif}} - V) = \frac{1}{2} m^* v_{00}^2. \quad (4)$$

Equation (3) can be evaluated analytically. However, it is important to realize that the current flowing in a small velocity interval Δv_x is given by

$$\Delta I = \text{Area}\frac{4\pi q m^{*2} k}{h^3} T v_x \exp\left(\frac{-\frac{1}{2}m^* v_x^2}{kT}\right) \Delta v_x. \quad (5)$$

This will be a useful result in the calculation of the noise.

For the dc current, the standard Richardson equation follows from (3). This yields

$$I = \text{Area}\, A^* T^2 \exp\left(\frac{-q\Phi_{ms}}{kT}\right) \exp\left(\frac{qV}{kT}\right) \quad (6)$$

where

$$A^* = \frac{4 q \pi m^* k^2}{h^3}. \quad (7)$$

The variations from the ideal case are adequately modeled by including a nonideality factor m in the expression for the diode current. A simplified expression of the diode current is

$$I = I_0\left(\exp\left(\frac{V}{m V_T}\right) - 1\right) \quad (8)$$

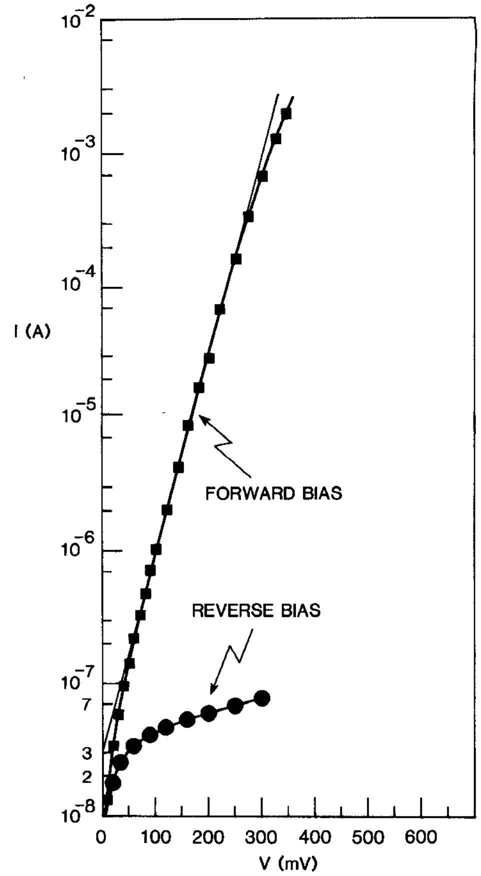

Fig. 3. $I-V$ characteristic of Hughes diode at 300 K.

where

$$I_0 = (\text{Area}) A^* T^2 \exp\left(\frac{-\Phi_{ms}}{V_T}\right) = I_s \exp\left(\frac{-V_{\text{dif}}}{V_T}\right). \quad (9)$$

The quantity I_s, which is defined by (9), will be convenient for use in the high-frequency analysis. Note that I_s is much greater than I_0. Also note that the constant reverse saturation current has now been included.

The measured $I-V$ characteristic of the Hughes model 47316H-1111 silicon Schottky-barrier diode detector is shown in Fig. 3. All measurements were performed at 300 K. The slope of the line indicates a nonideality factor m equal to 1.09. By extrapolating to zero bias, the reverse saturation current is found to equal 3×10^{-8}A. Assuming a junction diameter of 2 μm, the actual Schottky-barrier height is determined to be 0.585 eV.

The saturation current and Schottky-barrier height are important parameters in the device model. Another important parameter, which is a parasitic effect, is the series resistance. This plays an important role at high bias currents for both the admittance and noise. The value of the series resistance is determined from the deviation of the measured $I-V$ curve from a true exponential curve at high bias. For a current of 2 mA, the deviation is 20 mV. This indicates that the series resistance is 10 Ω.

The device parameters determined in this section will be used in the description of the noise properties. The measured values were used without modification.

IV. Intermediate-Frequency Theory

The intermediate-frequency noise theory has been known for some time [4]. The basic starting point of an analysis is the dc current, which one assumes can be described in the form of (8).

Assuming that the current I_d gives full shot noise and that the device conductance g_d is given by the derivative of the $I-V$ relationship when evaluated at the operating point, one obtains

$$S_I(f) = 4kT_n g_d = 2qI_{eq} = 2q(I+2I_0) \tag{10}$$

with $g_d = dI/dV = (I+I_0)/mV_T$.

From (10), the expression for T_n results in

$$T_n = \frac{mT}{2}\left(\frac{I+2I_0}{I+I_0}\right) \simeq \frac{mT}{2} \quad \text{for } I \gg I_0. \tag{11}$$

This is the well-known intermediate-frequency result and is commonly used. Note that it does not depend on bias under the stated assumptions. It is a common misconception that these devices will shown both thermal noise and shot noise when forward biased. In fact, the shot noise is the actual measured quantity. Even though the device has a known impedance, it is not a passive resistor at 300 K; rather, it is an active device. Since the device is not in thermal equilibrium, it is not necessary for it to give thermal noise.

Now consider the addition of a series resistance to the device model, as shown in Fig. 4.

In a measurement, only $S_{I_{eq}}$ can be determined, and this has a value of

$$S_{I_{eq}} = \frac{2qI_d r_j^2}{(r_s+r_j)^2} + \frac{4kTr_s}{(r_s+r_j)^2}. \tag{12}$$

This may be expressed in terms of a noise temperature as

$$T_n = \frac{2qI_d}{4k}\frac{r_j^2}{r_s+r_j} + \frac{Tr_s}{r_s+r_j}. \tag{13}$$

The results of the noise measurements between 10 Hz and 150 MHz are presented in Fig. 5. It is seen that the Hughes diode exhibits excess noise at low frequencies and then reaches a constant noise level for higher frequencies. The low-frequency noise goes approximately as $1/f$. The constant value which is reached corresponds closely to the calculated values for the shot noise of the bias current when the effect of the series resistance is included (see (12)). The calculated values are indicated by the solid lines, and these correspond to a noise temperature of $mT/2$.

Above the excess noise corner frequency, the theoretical shot noise level of the dc current coincides well with the measured noise level (see Fig. 6). This is true for the various bias currents which were used during the noise measurements. These shot noise measurements indicate that the device behaves in the well-known manner at intermediate frequencies.

In addition, Fig. 6 shows that there are no excess noise sources which extend into the microwave-frequency region.

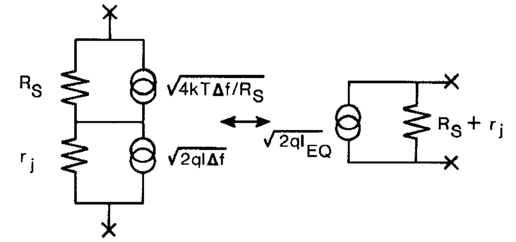

Fig. 4. Low-frequency model of a Schottky-barrier diode.

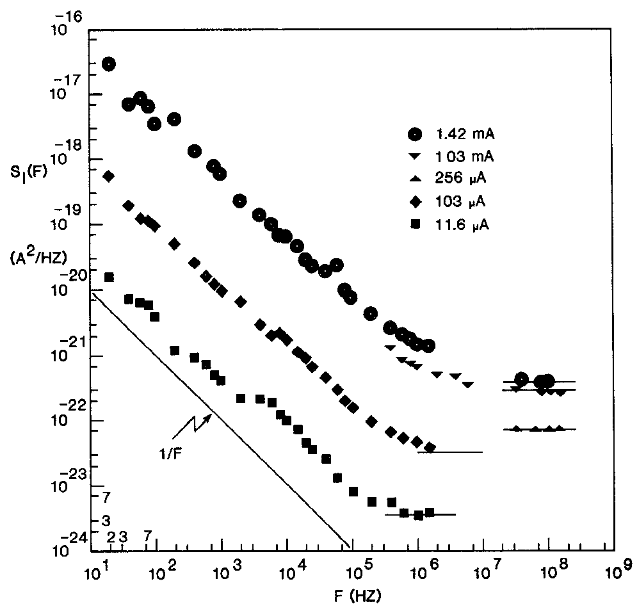

Fig. 5. Spectral intensity of current fluctuation versus frequency for the Hughes Schottky-barrier diode.

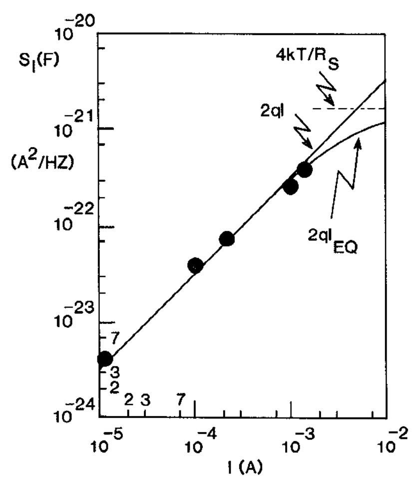

Fig. 6. Noise plateau values as a function of bias.

V. High-Frequency Theory

Van der Ziel has provided the theoretical framework for analyzing the effect of the transit time on Schottky-barrier diodes operating in the thermionic mode [5]. The case to be considered is for a uniformly doped semiconductor (linearly varying electric field). It is assumed that all of the electrons are emitted from the interface between the depleted/nondepleted region of the semiconductor.

In order to calculate the noise temperature of the device, the conductance and spectral intensity of the current pulse due to each electron must first be found. From the equations of motion, the velocity of an electron as a function of time may be found for an electron of any group. This velocity relates directly to the current flowing

$$i(t) = \frac{-qv(t)}{d} \tag{14}$$

where d is the width of the space-charge region.

From the equation of motion for a single electron, one finds

$$v_x(t) = v_x(0)\cos at \tag{15}$$

where a is the plasma frequency in radians per second and is equal to $(qE_{\max}/m^*d)^{1/2}$. Both $E_{\max}$ and d are functions of the applied bias. It should be noted that a small effective mass, such as for GaAs, leads to a shorter transit time and better high-frequency performances of the device.

Electrons which belong to group 1 have insufficient kinetic energy to cross the barrier and return to the undepleted semiconductor region. During their time of flight, the current which flows has the time dependence illustrated in Fig. 7. This is shown for the case of a single electron, but in practice the amplitude must be multiplied by the number of electrons injected with the same initial velocity.

The electrons of group 1, regardless of their initial velocity upon entering the space-charge region, all require the same characteristic time to return to the neutral semiconductor region. Only the amplitude of the current pulse changes due to the different possible initial velocities. The characteristic time for an electron to return is

$$\tau_R = \pi/a. \tag{16}$$

These electrons carry no dc current and at low frequencies do not give any significant contribution to the device admittance. The characteristic frequency associated with the current pulses is $f_R = 1/(2\pi\tau_R)$. When operated at high frequencies, the applied signal may be of a frequency on the same order of magnitude as this characteristic frequency. These current pulses thus give a contribution to the device admittance. The real part of this admittance component (i.e., the conductance) increases as ω^2 for low frequencies and reaches a maximum when the frequency of operation corresponds to 1.37 times f_R. The maximum may be found by differentiating the expression for the conductance. The conductance due to these electrons is given in [5] as

$$g_{11} = \frac{I_s - I_d}{V_{\text{dif}} - V_d}\frac{1}{2}\frac{c}{1-c^2} \cdot \left(\frac{1-\cos\pi(1-c)}{1-c} - \frac{1-\cos\pi(1+c)}{1+c}\right) \tag{17}$$

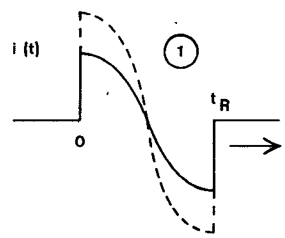

Fig. 7. The solid curve indicates the current pulse due to a single electron of group 1. The dashed curve is for an electron of slightly higher initial velocity. This figure shows that all electrons of group 1 have the same characteristic time of flight.

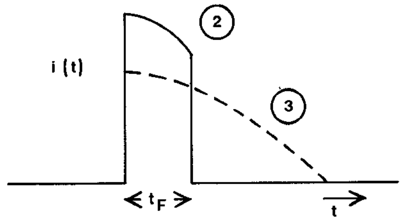

Fig. 8. The current which flows as a function of time caused by an electron of group 2 or group 3.

where the parameter c is the normalized angular frequency (defined as ω/a, where ω is the frequency of operation) and I_s was defined in (9). In this notation, I_s is very much larger than I_d for normal operation. This conductance dominates at high frequencies when the diode is operated at low bias currents. It should be recalled that most electrons have energies near the bottom of the conduction band edge and thus belong to group 1.

If the series resistance of the device is zero, then it is possible to calculate the effective noise temperature of the device with no knowledge of the junction susceptance. However, for most diodes the series resistance is not negligible, especially for high bias currents. The combined effect of the series resistance and junction susceptance will be discussed during the calculation of the theoretical noise temperature.

The component of junction susceptance due to those electrons which return can be found to equal [5]

$$b_{11} = \frac{I_s - I_d}{V_{\text{dif}} - V_d}\frac{c\pi}{2}\left[1 - \frac{\sin(1-c)\pi}{1-c} + \frac{\sin(1+c)\pi}{1+c}\right]. \tag{18}$$

The electrons with sufficient kinetic energy to always reach the metal contact are those of group 2. The current pulses due to two possible initial velocities are illustrated in Fig. 8. The device admittance is found by applying a small ac voltage and calculating the response of the electron velocity. The transit time is also changed due to the applied signal.

Since the electrons from this group are always collected, they carry the dc current and are not much affected by an applied small-signal voltage (dI/dV being approximately zero for this group of electrons). Nonetheless, an applied signal does influence the velocity of electrons during the transit time, and the contribution to the conductance may be calculated as

$$g_{22} = \frac{I_d}{V_{\text{dif}} - V_d} \int_0^\infty \exp - \left(\frac{eV_0'}{kT} \right) d\left(\frac{eV_0'}{kT} \right) \cdot \frac{1}{2} \frac{c}{1-c^2} \left(\sin\phi \sin c\phi + \frac{(1-\cos(1-c)\phi)}{1-c} - \frac{(1-\cos(1+c)\phi)}{1+c} \right) \tag{19}$$

where $\phi = a\tau_F$, eV_0' is the energy of the arriving electrons, and τ_F is the dc transit time.

Again, the component of device susceptance may be calculated and is equal to

$$b_{22} = \frac{I_d}{V_{\text{dif}} - V_d} \int_0^\infty \exp - \left(\frac{eV_0'}{kT} \right) d\left(\frac{eV_0'}{kT} \right) \cdot \frac{1}{2} \frac{c}{1-c^2} \left[\phi + \sin\phi \cos c\phi + \left(\frac{\sin(1-c)\phi}{1-c} + \frac{\sin(1+c)\phi}{1+c} \right) \right]. \tag{20}$$

It should be noted that, for most cases, the effect of electrons of this group may be ignored in the admittance calculation. However, in the calculation of the spectral intensity of the current fluctuations, the electrons of group 2 play an important role.

The final group of electrons which must be considered comprises those with barely sufficient energy to reach the metal contact. These electrons dominate the device conductance at low frequencies. Their contribution to the junction conductance is

$$g_{33} = g_0 \frac{\left(1 - 2c \sin \frac{1}{2} c\pi - c^2 \cos c\pi\right)}{(1-c^2)^2} \tag{21}$$

where g_0 is the low-frequency small-signal conductance.

The contribution to the device susceptance is

$$b_{33} = g_0 \frac{\left(c^2 \sin \pi c - 2c \cos \frac{\pi c}{2} \right)}{(1-c^2)^2}. \tag{22}$$

The total junction admittance is found from a superposition of the effects of the three groups of electrons. At low frequencies, the admittance has only a real part. This conductance is due to the electrons of group 3 and is the same result as obtained from the derivative of the $I-V$ relationship. The calculation of the derivative is analogous to evaluating the change in the number of electrons which cross the barrier when a signal is applied. Since only the number of electrons in group 3 is modulated, they give the low-frequency junction conductance.

VI. Calculation of the Spectral Intensities

In order to calculate the noise temperature of the diode, the spectral intensities of the current fluctuations due to each group of electrons must be calculated. The total spectral intensity is found by summing the contribution of each electron. It should be noted that the calculation of the spectral intensity can proceed by considering only two cases: electrons which can cross the space-charge region and those which cannot. The electrons of group 3 always cross the barrier in the absence of an applied signal. Since the spectral intensity is calculated for the case of an ac short circuit, groups 2 and 3 may be combined.

The calculation of the spectral intensities follows along straightforward lines but involves lengthy expressions. The procedure is as follows: 1) calculate the current which flows as a function of time for a given initial velocity of an electron; 2) take the Fourier transform of the current pulse due to electrons with this initial velocity; 3) calculate the number of electrons flowing with this velocity; 4) apply Carson's theorem [6] using results 1–3 in order to find the spectral intensity for a particular initial velocity; and 5) sum over all possible initial velocities in order to find the total spectral intensity.

The first case which will be considered is for electrons which reach the metal contact. The time of flight τ_F is found from the equation of motion and is equal to

$$\tau_F = 1/a \arcsin\left(ad/v_x(0)\right). \tag{23}$$

Since the velocity of the electron as a function of time is known, the current which is flowing is also known [6]. The Fourier transform of this current pulse is needed in order to calculate the current spectral intensity and is equal to

$$\psi = \int_{-\infty}^{\infty} \frac{-qv_x(0)}{d} \cos at\, e^{-j\omega t}\, dt = j\frac{C_1}{a} \left\{ \frac{1}{1+c} \left(e^{-j(1+c)a\tau_F} - 1\right) - \frac{1}{1-c} \left(e^{j(1-c)a\tau_F} - 1\right) \right\} \tag{24}$$

where $C_1 = qv_x(0)/2d$.

The spectral intensity due to the electrons which cross with this initial velocity is found by using Carson's theorem

$$\Delta S_{I_{22}}(f) = 2\lambda\psi\psi^* \tag{25}$$

where λ is the average number of electrons being emitted per unit time with a given velocity. The spectral intensity $\Delta S_{I_{22}}$ is that due to the electrons in a small velocity interval centered about $v_x(0)$.

A calculation of lambda follows from the dc current. Let $\Delta I_{22}(K)$ be the current flowing in a velocity interval $\Delta v_x(K)$ as defined by (5). The index K denotes the particular velocity interval under consideration. The size of the intervals is chosen in such a way that the final results of our computer calculations are accurate within one-tenth of a percent. The quantity lambda is the average rate at which emissions are occurring. Hence

$$\lambda(K) = \Delta I_{22}/q. \tag{26}$$

Now that all of the necessary quantities have been evaluated, the total spectral intensity $S_{I_{22}}$ is calculated by summing over all velocity intervals. This yields

$$S_{I_{22}}=\sum_K \frac{2\lambda(K)C_1^2}{a^2}\frac{2}{(1+c)(1-c)}\Big\{(1-\cos(1-c)\cdot a\tau_F(K))\frac{2c}{1-c}-(1-\cos(1+c)a\tau_F(K))\frac{2c}{1+c}+(1-\cos 2a\tau_F(K))\Big\} \quad (27)$$

where the index K again refers to a particular small-velocity interval. It should be kept in mind that $\tau_F(K)$ is the transit time of an electron in the small-velocity interval under consideration.

Since the case being considered is for the electrons which are able to cross the junction, the summation should start at a velocity of v_{00} and go to infinity. The value of v_{00} is found from the minimum kinetic energy required to cross the barrier of the junction. This is obtained from (4). In practice, the summation only needs to be carried out over a few kT of energy.

The second case, that of electrons which have insufficient kinetic energy in order to cross the junction, is considered in the same manner.

Again, the calculation begins by taking the Fourier transform of a single current pulse. The results of the previous calculation may be used if it is kept in mind that τ_F should be replaced everywhere by τ_R (see (15)). The resulting expression may be simplified, using trigonometric identities, to the following form:

$$\psi\psi^*=\frac{C_1^2}{a^2}\frac{8c^2}{(1-c^2)^2}(1+\cos c\pi). \quad (28)$$

The calculation of the total spectral intensity $S_{I_{11}}$ is similar to the calculation of $S_{I_{22}}$, except that the limits of evaluation need to be changed for this group of electrons. Electrons at the bottom of the conduction band have only potential energy and no kinetic energy. Thus, the lower limit of evaluation is $v_x(0)=0$. Electrons which almost reach the metal contact, yet fail, have an initial velocity equal to v_{00}, as defined by (4).

The total spectral intensity of those electrons which do not reach the metal contact and then return to the neutral semiconductor becomes

$$S_{I_{11}}(f)=\sum_K \Delta S_{I_{11}}=\sum_K \frac{2\lambda(K)C_1^2}{a^2}\frac{8c^2}{(1-c^2)^2}(1+\cos c\pi). \quad (29)$$

The spectral intensity of current fluctuations due to the electrons of group 1 is shown by the dashed curves in Fig. 9. The noise of these electrons which return is zero for zero frequency, since these electrons carry no dc current. The spectral intensity is seen to rise initially as f^2.

The lower curve is for a bias voltage of five times V_T and the upper curve is for a bias voltage of ten times V_T. This illustrates that the spectral intensity due to electrons of group 1 is a very slow function of the bias.

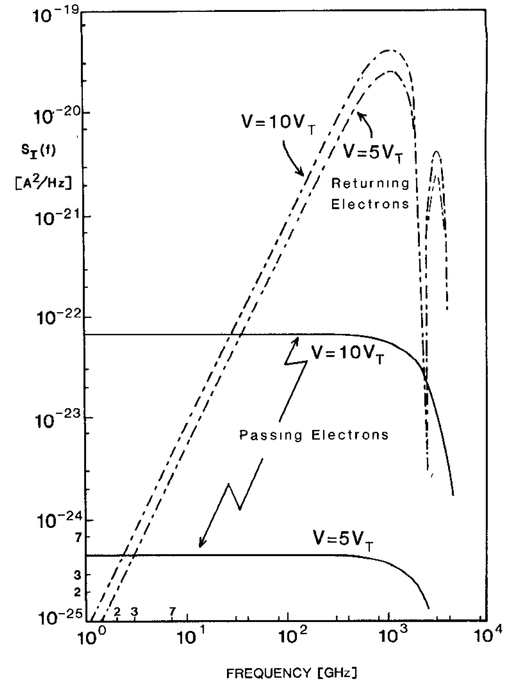

Fig. 9. Spectral intensities versus frequency. The lower solid and dashed curves are for $V_d=5\ V_T$, whereas the upper solid and dashed curves are for $V_d=10\ V_T$. V_T is the thermal voltage and is equal to 25.8 mV at room temperature.

Since all electrons of this group have the same characteristic time of flight, the spectral intensity shows several sharp nulls. This would not be the case if the time of flight took on a distribution of values as in the case of, for example, a uniform electric field.

The spectral intensity due to the passing electrons, groups 2 and 3, is illustrated in Fig. 9 by the solid curves and is equal to the shot noise of the dc current at low frequencies. At frequencies on the order of the reciprocal transit time, the spectral intensity falls off steeply. The lower solid curve is for a bias voltage of five times V_T and the upper curve is for a bias voltage of ten times V_T. It is clear that this component of the spectral intensity is a very strong function of the applied bias.

For a given frequency of operation, e.g., 12 GHz, it may now be seen that there are two distinct regimes of operation. At low bias the noise of the returning electrons is dominant, while at high bias the noise of the passing electrons becomes dominant. Furthermore, the higher the frequency of operation, the higher the bias must be in order for the passing electrons to dominate the noise.

VII. Calculation of the Noise Temperature

The noise temperature is calculated as a function of both bias and operating frequency by combining the various components of device conductance and spectral intensity as follows:

$$T_n=\frac{S_{I_{\rm jnc}}(f)}{4kg_{\rm jnc}} \quad (30)$$

where g_{jnc} is the total junction conductance from all groups of electrons and $S_{I_{jnc}}(f)$ is the spectral intensity of current fluctuations due to all groups of electrons.

Consider the case of a junction with nonideality factor of unity and no parasitic resistances or capacitances. If only the passing electrons are considered, then the noise temperature would be equal to half the ambient temperature. This is the standard result for intermediate frequencies, where the returning electrons may be neglected.

For low-bias operation at high frequencies, the returning electrons may not be neglected. This group of electrons has a noise temperature associated with it which is equal to the ambient temperature. As the bias is increased, the passing electrons begin to dominate the device behavior, and the noise temperature again drops to half the ambient temperature.

The description of the junction presented so far has only been concerned with an ideal exponential junction. In practice this is not sufficient as the effects of the series resistance, diode nonideality factor, and reverse saturation current must also be considered in an actual device.

In most cases, the series resistance is of the greatest concern. This resistance degrades the performance of the device in every manner. Due to the series resistance, rectification properties are reduced, matching to the actual junction becomes difficult, and, in general, the effective noise temperature of the diode is increased. The series resistance can be appreciable in microwave diodes due to the small metal contact area which is used (typically 2 μm diameter).

At very high bias levels, the series resistance may be the source of excess noise. At high frequencies, the effective series resistance may be greater than that obtained from $I-V$ measurements due to the skin effect. It is difficult to accurately model the series resistance for high-bias and high-frequency operation [7]. In this work, it will be assumed that the series resistance is constant and equal to its low-frequency value. The intermediate-frequency noise data which are presented in Fig. 6 clearly show that hot electron effects in the series resistance of the diode are absent at the bias currents which were used in our experiments. Consequently, the noise temperature of the series resistance is equal to the ambient temperature.

The diode nonideality factor was assumed to be equal to unity in these calculations. For the diode which was measured this is a reasonable assumption since it was found experimentally that $m = 1.09$. At worst, this gives an error of 9 percent in the noise temperature. The nonideality factor could be taken into account by recalculating the Schottky-barrier height for each bias point. This would lead to a different value of the minimum velocity required for an electron to reach the metal contact.

At very low values of bias ($V_d < 5mkT/q$), it is important to include the reverse saturation current in the device model. If this current is omitted, then the calculated current for zero applied voltage would be nonzero, and the noise temperature would not match the ambient temperature, as it should.

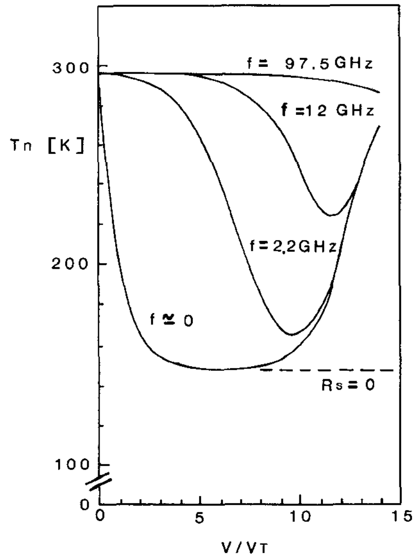

Fig. 10. Theoretical noise temperature versus bias voltage.

The results of the theoretical calculations of T_n are presented in Fig. 10. The curves of Fig. 10 indicate that for each frequency of operation there is an optimum bias. It is at this bias that the lowest noise temperature of the diode will be obtained. The lowest noise temperature which can be achieved increases with the operating frequency. At high frequencies, the lowest noise temperature is not much lower than the ambient temperature.

At low frequencies, with no series resistance, the effective noise temperature is 295 K at zero bias and drops sharply to 147.5 K. This is the well-known result for intermediate frequencies. By including the series resistance of 10 Ω, it can be seen that for high biases the series resistance dominates over the junction resistance and the noise temperature again rises to the effective temperature of the series resistance.

When operated at high frequencies, the noise temperature does not begin to drop until a higher bias is reached. This is due to the fact that at low bias the noise and conductance of the device are dominated by the returning electrons. At high frequencies, the noise temperature of the diode remains nearly constant due to the returning electrons. At 97.5 GHz, there is almost no decrease in the noise temperature.

The rolloff from the ambient temperature towards a noise temperature of $mT/2$ occurs when the spectral density and conductance of the passing electrons dominate. The bias at which the rolloff beings is a function of frequency. If there were no series resistance, then the noise temperature would always reach a value of $mT/2$, even at high frequencies.

At 2.2 GHz, the high-bias portion of the curve is seen to be dominated by the series resistance. It should be recalled that at low bias the returning electrons cause both the junction conductance and susceptance to be large compared to their low-frequency values. This allows the series resistance to play a role even at the lower biases. The series resistance, in conjunction with the junction susceptance,

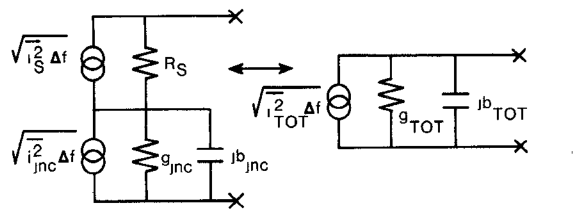

Fig. 11. Circuit transformation which includes the effects of the series resistance and junction susceptance.

causes the effective conductance at the device terminals to be increased. The circuit transformation which is made is indicated in Fig. 11. It is the transformed quantities which are measured.

VIII. High-Frequency Measurements

The noise measurements were performed on a Hughes silicon diode detector (model 47316H-1111) using the circulator method of Gasquet *et al.* [8]. Since four measurements are performed, there are also four quantities which can be determined. It is possible to determine T_a, the system background noise temperature; $K \cdot G \cdot B$, the gain–bandwidth product (K is a constant of proportionality); T_{DUT}, the device under test noise temperature; and $|\Gamma|^2$, the magnitude of the reflection coefficient squared. Usually, only the last two quantities are of interest.

Microwave measurements were performed at 2.2, 12, and 97.5 GHz. The receiver front end used at 97.5 GHz is shown in Fig. 12. The front ends for use at 2.2 and 12 GHz were similar but used low-noise amplifiers instead of the mixer. The down conversion and detection were done using the setup shown in Fig. 13. This portion of the circuit was the same for all of the measurements, although an HP desktop computer was used to record the voltmeter readings during 97.5-GHz noise measurements. Use of the computer allows for long averaging times to obtain the required statistical accuracy.

IX. Measurement Results and Discussion

The results of the noise measurements are presented in Fig. 14. They are seen to be in good agreement with the theoretical results which were presented earlier.

In equilibrium, the noise temperature of the device is equal to the ambient temperature for all frequencies. At 2.2 GHz, the noise temperature begins to roll off at five times V_T. For a frequency of 12 GHz, the rolloff does not begin until eight times V_T. There is almost no decrease in the noise temperature of the diode at 97.5 GHz. This shows the region where the group of returning electrons is dominant.

In the rolloff region, the noise temperature is dropping due to the group of passing electrons. The noise temperature which is associated with the electrons of groups 2 and 3 is half of the ambient temperature. The lowest noise temperature which is reached at 2.2 GHz is 180 K. This is reasonable considering that the value predicted by the model is 165 K. The theoretical model ($m = 1$) always gives a noise temperature which is slightly lower than the actual noise temperature. This is due to the neglect of the diode

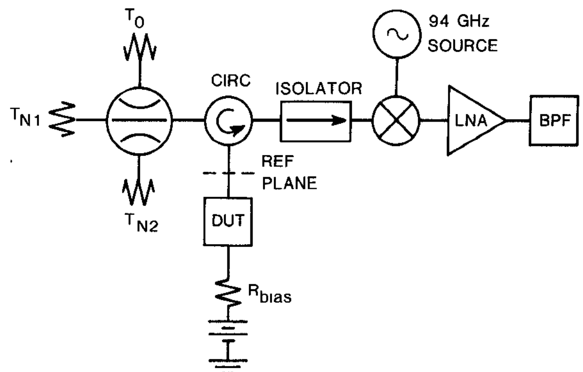

Fig. 12. Front end of the noise measurement setup for 97.5 GHz.

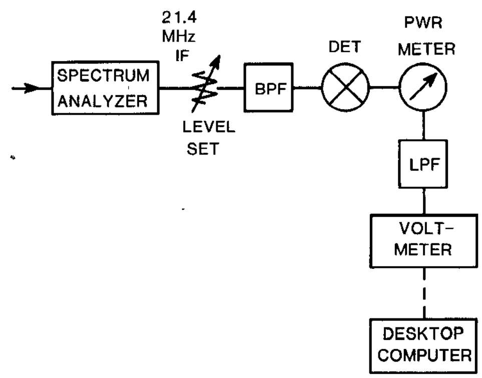

Fig. 13. Detection system for noise measurements. The desktop computer was needed only during 97.5-GHz measurements.

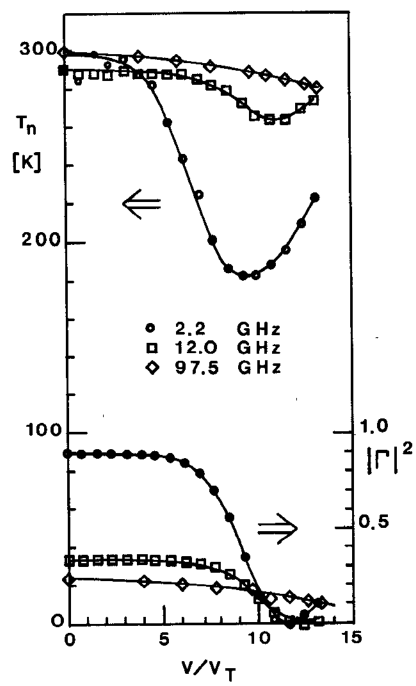

Fig. 14. Noise temperature versus bias for the Hughes Schottky-barrier silicon diode.

nonideality factor and causes an error of, at most, 9 percent (14 K).

At high bias, the noise temperature rises sharply but never exceeds the ambient temperature. This indicates that hot-electron effects and excess noise sources are negligible in this current range. The increase in T_n is due to the series resistance.

The measured reflection coefficient as a function of the bias and frequency of operation is also shown in Fig. 14. It is seen from these results that transit-time effects also influence the conductance of the device at high frequencies.

X. Conclusions

A high-frequency device model of Schottky-barrier diodes which takes into account the distribution of electron velocities has been presented. The initial velocities of electrons from the semiconductor upon entering the junction space-charge region have been divided into three regimes, and in each regime the effect of the transit time has been calculated. In addition, a fourth group of electrons traveling from the metal to the semiconductor and the effects of the series resistance on the noise spectrum were included in the calculation.

In order to prove that the final high-frequency results were due to transit-time effects, it was necessary to show that the diode behaved in the well-known manner at intermediate frequencies.

The high-frequency noise measurements were performed at 2.2, 12, and 97.5 GHz to study the transit-time effects as a function of frequency. The results of the measurements are in good agreement with the device model presented.

References

[1] M. T. Faber, J. W. Archer, and R. J. Mattauch, "A very low noise, fixed tuned mixer for 240–270 GHz," in *IEEE MTT-S Int. Microwave Symp. Dig.*, 1985, p. 311.

[2] S. M. Sze, *Physics of Semiconductor Devices*, 2nd ed. Englewood Cliffs, NJ: Prentice-Hall, 1981, p. 262.

[3] A. van der Ziel, *Solid State Physical Electronics*, 2nd ed: Englewood Cliffs, NJ: Prentice-Hall, 1968.

[4] B. M. Oliver, "Thermal and quantum noise," *Proc. IEEE*, vol. 53, no. 5, p. 436, 1965.

[5] A. van der Ziel, "Infrared detection and mixing in heavily doped Schottky-barrier diodes," *J. App. Phys.* vol. 47, no. 5, p. 2059, 1976.

[6] A. van der Ziel, *Noise in Measurements*. New York: Wiley, 1976, p. 42.

[7] D. N. Held and A. R. Kerr, "Conversion loss and noise of microwave and millimeter-wave mixers: Part 2—Experiment," *IEEE Trans. Microwave Theory Tech.*, vol. MTT-26, no. 2, p. 55, 1978.

[8] D. Gasquet, J. C. Vaissiere, and J. P. Nougier, "New method for wide band measurement of noise temperature of one-port networks at high pulsed bias," in *Sixth Inter. Conf. on Noise in Physical Systems, NBS Special Publication*, vol. 614, 1981, p. 305.

Michael Trippe (S'85–M'85) was born on September 7, 1957. He received the B.S., M.E., and Ph.D. degrees in electrical engineering from the University of Florida, Gainesville, FL, in 1979, 1981, and 1986, respectively.

His interests include the modeling, characterization, and testing of solid-state devices and materials for use at microwave and millimeter-wave frequencies. He is currently employed at Martin Marietta Laboratories, Baltimore, MD.

Dr. Trippe is a member of Tau Beta Pi, Eta Kappa Nu, and Phi Kappa Phi.

Gijs Bosman (M'82) received the B.S., M.A., and Ph.D. degrees in physics from the State University of Utrecht, The Netherlands, in 1971, 1976, and 1981, respectively.

Since 1981, he has been Assistant Professor of electrical engineering at the University of Florida. His research interests include electrical noise in various devices, hot-electron phenomena, and the charge-transport properties of submicrometer devices and of two-dimensional electron gases.

Dr. Bosman is a member of the Dutch Physical Society.

Aldert van der Ziel (SM'49–F'56–LF'81) was born in Zandeweer, The Netherlands, on December 12, 1910. He received the Ph.D. degree in physics from the University of Groningen, The Netherlands, in 1934.

He was a member of the research staff of the laboratory of the N.V. Philips Gloeilampenfabrieken in Eindhoven, The Netherlands, from 1934 to 1947, working on vacuum-tube and noise problems. From 1947 to 1950, he was Associate Professor of physics at the University of British Columbia, Vancouver, B.C., Canada. Since 1950, he has been Professor of electrical engineering at the University of Minnesota, Minneapolis. Since 1968, he has been a part-time Graduate Research Professor at the University of Florida, Gainesville.

Dr. van der Ziel received the Western Electric Award of the A.S.E.E. in 1967, the Vincent Bendix Award of the A.S.E.E. in 1975, and the IEEE Education Medal in 1980. He has also received honorary doctor's degrees from the Universite Paul Sabatier, Toulouse, France, 1975, and from the Eindhoven University of Technology, Eindhoven, The Netherlands, 1981.